

1 **Salinity increases with water table elevation at the boundary**

2 **between salt marsh and forest**

3 Giovanna Nordio¹, Sergio Fagherazzi¹

4 ¹Department of Earth and Environment, Boston University, Boston, MA USA

5 **Abstract**

6 The migration of salt marshes into forests along coastal regions is nowadays well documented. Sea
7 level rise and storms threaten coastal forests by increasing groundwater levels and salinity.
8 Salinization is the main cause of forest conversion to salt marsh in North America. In this paper
9 we study groundwater levels and salinity in two wells installed at the border between forest and
10 salt marsh in the lower Delmarva peninsula, USA. The upper well is located in the regenerative
11 forest, where recruitment is still possible, while the lower well is located in the persistent forest,
12 where only mature trees survive. Groundwater in the upper well is fresh at the roots depth, while
13 in the lower well the mean salinity is 8 ppt. Our data suggest that rainfall has an instantaneous
14 effect on salinity and groundwater levels, but it does not affect salinity and groundwater levels on
15 longer periods (weeks to months). Groundwater levels and salinity reflect the hydraulic gradient
16 toward the marsh (a proxy for outgoing water fluxes), the uphill hydraulic gradient (a proxy for
17 incoming water fluxes) and temperature (a proxy for evapotranspiration). Salinity increases when
18 groundwater levels are high. To explain this result, we put forward the hypothesis that a high water
19 table favors the flux of surficial, fresh water to the marsh, and loss of freshwater by
20 evapotranspiration. These losses are likely replenished by saltier water moving at depth.

21 **1. Introduction**

22 Freshwater availability, flooding and soil salinity can be considered the main drivers of ecological
23 zonation in many coastal regions (Thibodeau et al. 1998; Gardner et al. 2002; Wilson et al. 2015).
24 In temperate areas, these factors play a crucial role in structuring the salt marsh-forest interface
25 (Fagherazzi et al. 2019). Being either not salt tolerant or not flood tolerant, coastal trees can be
26 killed by increasing tidal flooding, leading to forest retreat and marsh expansion. Coastal forest
27 retreat is generally driven by sea-level rise and storm events that affect the marsh-upland boundary
28 at different spatial and temporal scales. Sea level rise progressively increases the salinity of coastal
29 zones, thus influencing vegetation recruitment (see Fagherazzi et al. 2019 for a review). Salt
30 intrusion in aquifers can also be exacerbated by water withdrawals in populated areas (Pezeshki et
31 al. 1990). Strong winds and storm surges, usually associated with tropical cyclones, can cause
32 short-term damages and killing of trees, making space available for new vegetation. According to
33 Duryea et al. (2007), strong winds are responsible for defoliation, breakage and uprooting of trees.
34 Storm surges cause saltwater intrusion that suppresses seed germination, suffocates and inhibits
35 root formation and tree survival (Fernandes et al. 2018). In general, tree seedlings are more
36 susceptible to salt and flooding than mature trees whereas storm events directly affect the survival
37 of all trees (Kearney et al. 2018).

38 Rainfall events can have a positive effect on the forest bordering a salt marsh, reducing
39 groundwater salinity by dilution (Sumner et al. 2005). However, as sea level increases, rainfalls
40 could flood soils causing tree mortality from anoxia (Stanturf et al., 2007). When occurring
41 simultaneously, rainfall and salt intrusion events result in specific dynamics. If the soil was already
42 saturated with fresh water before a storm surge, it is unlikely that groundwater salinity increases
43 (Gardner et al. 1992, Allen et al. 1996). Flooding events affect the available oxygen content in the
44 soil, decrease the soil redox potential, and consequently slow the photosynthetic activity in flood

45 intolerant vegetation species (Anderson and Pezeshki 1999). Salt intrusion in the soil undermines
46 the growth of new leaves and accelerate the senescence of mature trees (Munns and Tester 2008).
47 Evapotranspiration is also a main hydrological driver in coastal forests. Evapotranspiration creates
48 an upward soil water flow with solute concentrating or precipitating near the soil surface, making
49 salt ions available to be absorbed by roots (Mohamed et al. 2000). The relationship among
50 precipitation, evapotranspiration, and tidal oscillations is fundamental to characterize groundwater
51 levels and salinity in a forest and adjacent salt marsh. Tidal inputs directly affect groundwater
52 discharge (Li and Berry 1999). When large storm surges occur, flooding often augment the salinity
53 of the soil, affecting vegetation growth. Salt intrusion can also reach deep ground layers and the
54 aquifer (Robinson et al 2007).

55 All hydrological inputs should be considered to determine groundwater dynamics during a storm.
56 Although many studies have focused on the marsh-upland boundary dynamics (Fagherazzi et al.
57 2019) or have analyzed and interpreted salinity data for these regions (Gardner et al. 2002, Carter
58 et al. 2008), the salinity dynamics at the marsh-upland interface remain unclear. The goal of this
59 paper is to characterize variations in groundwater level and salinity in a coastal forest bordering a
60 salt marsh. We will explore how rainfall, evapotranspiration, and storm surges might control both
61 water levels and salinity for two wells. Our preliminary results indicate that groundwater dynamics
62 at the marsh/forest interface can be complex and therefore will require extensive field campaigns
63 in the future.

64 **2. Study area**

65 We focus our study on a coastal forest in the Eastern Shore of Virginia National Wildlife Refuge
66 on the southern tip of the Delmarva Peninsula, in Virginia, United States (Fig. 1). The Delmarva
67 Peninsula is bordered by the Atlantic Ocean on the eastern side and by Chesapeake Bay on the

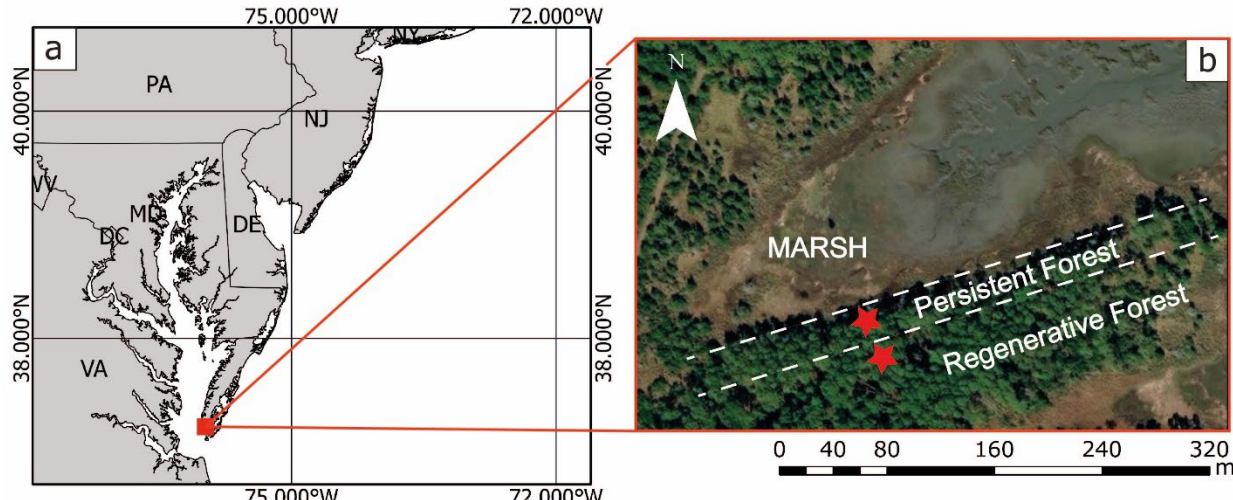
68 western and southern sides. This area is experiencing particularly high rates of sea level rise,
69 around 5 mm/yr (Sallenger et al. 2012). The forest is dominated by loblolly pine (*Pinus taeda*),
70 particularly common in the southeastern regions of the United States. At the salt marsh boundary,
71 the forest changes to a woody shrubs zone, characterized by *Juniperus virginiana*, *Iva frutescens*,
72 *Baccharis halimifolia* and *Myrica cerifera* (Fernandes et al. 2018). This zone borders, in turn, a
73 salt marsh ecosystem, where *Spartina alterniflora* is the most representative species. The
74 Delmarva peninsula climate varies between humid subtropical to the south, characteristic of
75 Eastern Virginia, to humid continental to the north, characteristic of Northern Delaware and North-
76 Eastern Maryland. The average annual maximum daily temperature in Cape Charles, close to our
77 study area, is 19.4 °C, while the average annual minimum daily temperature is 10.6 °C. The
78 average annual rainfall is around 1140 mm.

79 The Delmarva peninsula experiences a semidiurnal tidal cycle, with a mean low tide (MLW) of -
80 0.40 cm and a mean high tide (MHW) of 0.393 cm on MSL at Kiptopeke station. The Delmarva
81 peninsula is often affected by tropical cyclones and winter Nor'Easters that can cause coastal
82 flooding. According to the Virginia Department of Emergency Management, the Delmarva
83 peninsula has been hit by some of the strongest storm events since 2003. On September 18th, 2003
84 during Hurricane Isabel, sea level reached 1.34 m on NAVD88 at the NOAA Kiptopeke station.
85 On November 13th, 2009 during Tropical Depression Ida and Nor'Easter, sea level reached 1.50
86 m. On August 27th, 2011 during Hurricane Irene, sea level reached 1.35 m and on October 29th,
87 2012 during Hurricane Sandy, sea level reached 1.48 m.

88 Over the years, storm events along with sea level rise have affected the ecological zonation of the
89 marsh-forest interface, establishing a higher regenerative zone, rich of saplings, and a lower
90 persistent forested zone, where only mature trees survive (Kearney et al. 2019). Sea level rise

91 advances the salt marsh in the forest, while storm events move the lower boundary of the
92 regenerative zone towards the upland. This ecological ratchet was fully described in Fagherazzi et
93 al. (2019).

94



95

96 *Figure 1: a) location of the study site in Virginia, USA, b) location of groundwater wells (red stars) (after the study*
97 *of Kearney et al. 2019).*

98

99 Data

100 Water level and conductivity were measured in two groundwater wells along a transect (Fig. 1b).
101 The transect starts at the marsh boundary to the north and ends in the middle of the forest; it was
102 chosen to be perpendicular to the gently sloping hillside reaching the regeneration zone.
103 A Schlumberger Water Service CTD diver, able to measure conductivity, temperature and water
104 depth was installed in each well. A first well was placed at the lowest boundary of the pine forest
105 in the persistent zone, where adult trees can survive but not saplings. The well is at $1.16 \text{ m} \pm 0.14$
106 m (lower well) and at a depth of 0.80 cm below the ground surface (elevation of 0.334 m on

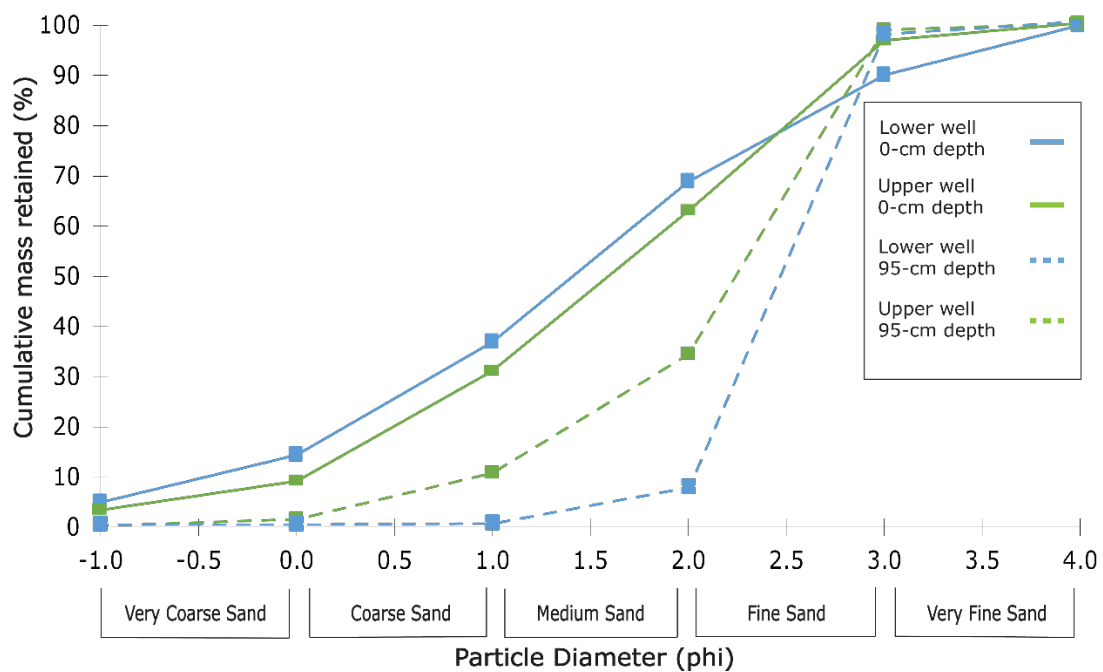
107 NADV88). The second well was placed at the line of sapling at the beginning of the regenerative
108 zone, at $1.24\text{ m} \pm 0.13\text{ m}$ (upper well) and at a depth of 0.90 m below the ground surface (elevation
109 of 0.507 m on NADV88). The wells were screened to the surface. According to McFarland and
110 Scott (2006) the approximate altitude of the top of bedrock basement is between -1500m and -
111 1800 m on NGVD29 (~NAVD88) in the Virginia Eastern shore. The general groundwater flow
112 direction is towards Chesapeake Bay (McFarland & Scott 2006). Well positions on a slope
113 (inclination angle estimated = 0.86 deg) suggest the general flow direction from the upper site to
114 the marsh. In 2013 mean Chesapeake forest age ranged from 16 to 40 years. According to Fire
115 Effects Information System (FEIS), *Pinus taeda* taproots grow between 1.2 to 1.5 m in depth.
116 Therefore, the CTD depth of around 0.80cm in the lower well corresponds to the mean root depth.

117 Hourly water level data were collected from 08 January 2014 to 07 January 2015, and referenced
118 to North American Vertical Datum 1988 (NAVD88). Hourly conductivity data were converted
119 into hourly water salinity data using the conductivity-salinity algorithm provided by Fofonoff and
120 Millard (1983), where data are reported in practical salinity scale 1978 (PSS78).

121 The soil of the study area has been characterized on the basis of cores collected in January, 2014.
122 For both lower well site and upper well site, six soil samples at depth of 0 cm, 20 cm, 40 cm, 60
123 cm, 80 cm and 95 cm were taken. The particles size was analyzed using a Ro-Tap sieve shaker
124 equipped with sieves of $2000\text{ }\mu\text{m}$, $1000\text{ }\mu\text{m}$, $500\text{ }\mu\text{m}$, $250\text{ }\mu\text{m}$, $125\text{ }\mu\text{m}$ and $63\text{ }\mu\text{m}$. Finally, obtained
125 data were processed using GRADISTATv8 program (Blott and Pye, 2001). Soil can be
126 homogeneously classified as moderately sorted medium-fine sandy in the study area (Fig. 2).

127 Available hourly precipitation data (mm/hr) were collected by the Virginia Coast Reserve Long
128 Term Ecological Research (VCR-LTER) at the Hog Island station (VCR97018). Because of the

129 38-kilometer distance between Hog Island station and the Eastern Shore of Virginia National
130 Wildlife Refuge, precipitation data collected at this station might not capture all rainfall events.
131 Daily temperature data collected at the same station are used to assess evapotranspiration effects
132 on groundwater levels. Evapotranspiration was estimated using temperature-based approaches
133 (Trajkovic 2005, Yates and Strzepe 1994), which might result in an overestimation in such humid
134 conditions if the model used is not correctly calibrated (Trajkovic 2007). Sea level data were
135 obtained from the NOAA Kiptopeke station (Identifier: 8632200). Kiptopeke station is located 5
136 kilometers from the study site, and the data are referred to NAVD88. Tidal data also capture storm
137 surges.



138

139 *Figure 2: Cumulative frequency curves of sediment diameter at the upper and lower well in 2014.*

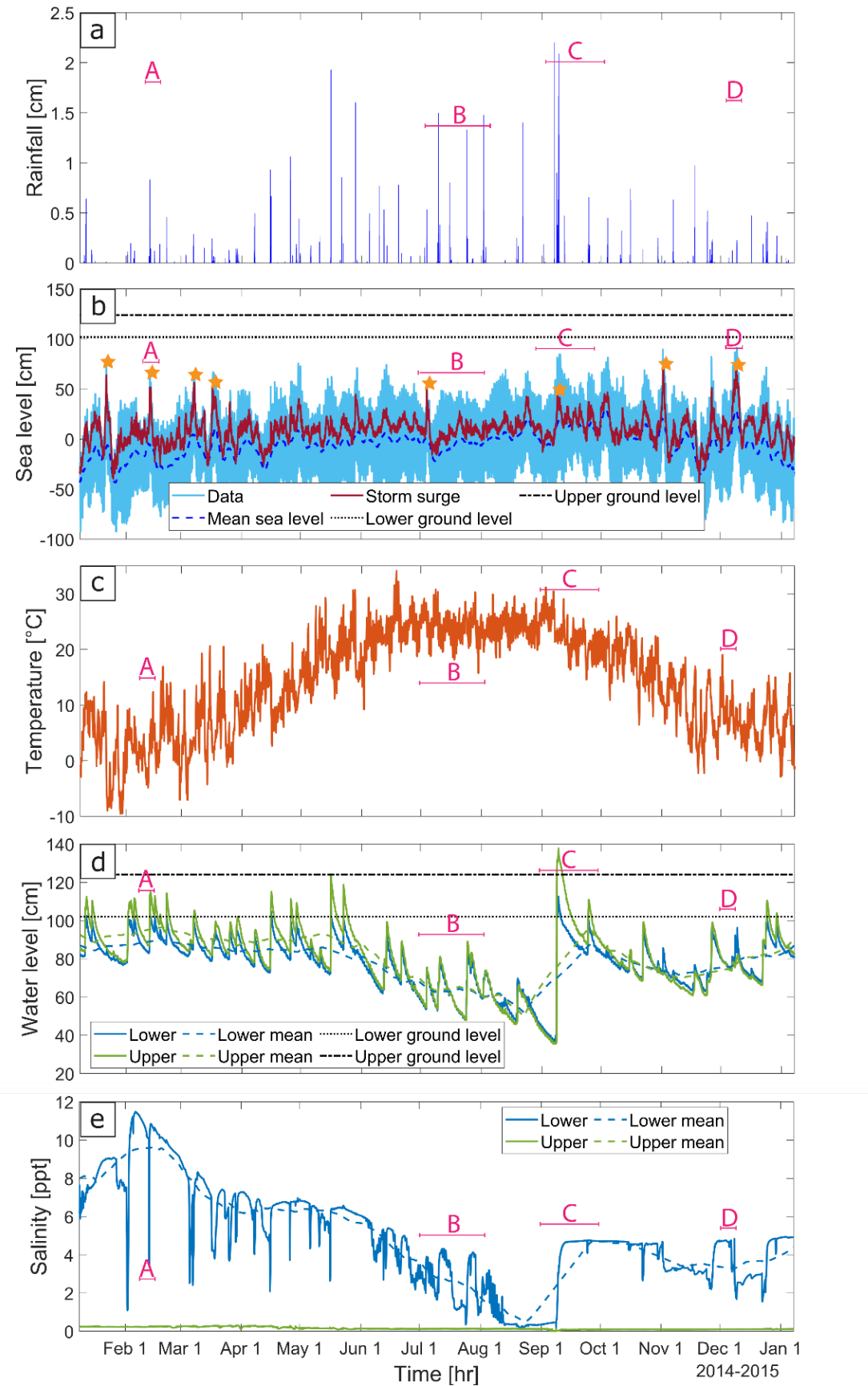
140

141 **3. Results**

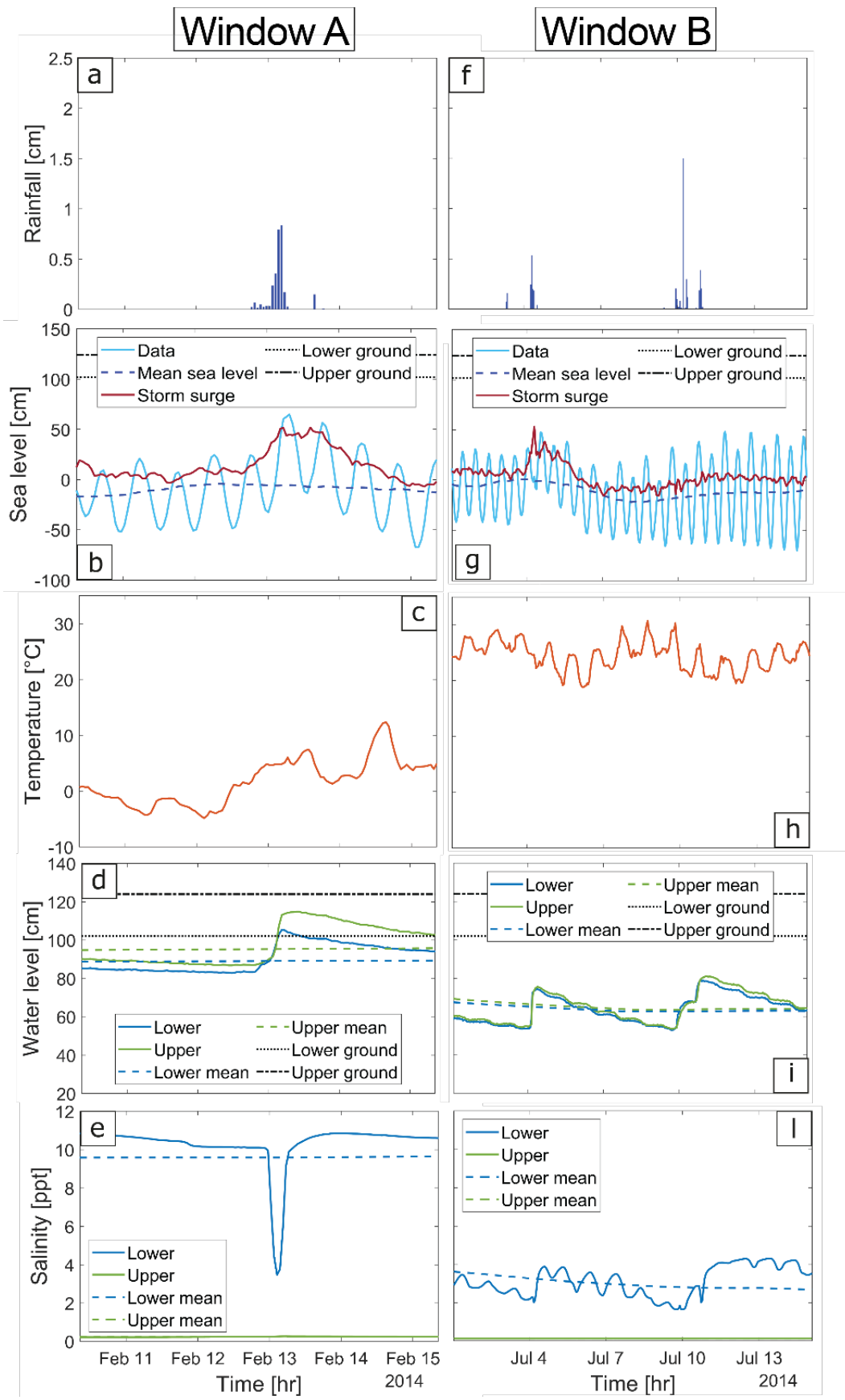
142 The groundwater table dynamics in both wells are similar (Fig. 3d), while salinity values indicate
143 a significant difference (Fig. 3e). According to Kearney et al. (2019), the groundwater table (Fig.
144 3d) is generally below the ground surface, except for few days, when either occasional heavy
145 rainfalls or long rainy periods occur (Fig. 3a). This happens several times during the year at the
146 lower well, on 11 January, 13 February, 16 April, 16 May, 8 September and 24 December when
147 the water level reaches the ground surface at 102 cm on NAVD88. On the other hand, flooding
148 only occurs in the upper well on 8 September, when the groundwater level reaches the ground
149 surface at 124 cm on NAVD88.

150 Overall groundwater table elevations vary from 36.9 cm to 112.6 cm above NAVD88 in the lower
151 well and from 35.5 cm to 137.8 cm in the upper well. In the lower well, closer to the salt marsh,
152 the salinity values are much higher than the values in the upper well. In particular, in the lower
153 well the salinity ranges from 0.13 to 11.48 ppt, while in the upper well the salinity ranges from
154 0.01 to 0.29 ppt (Fig. 3e). A moving average carried out considering a window of 800 hours
155 highlights the seasonal trend of groundwater table and groundwater salinity (Fig. 3d-e).

156 The most conspicuous precipitation events occur from April to September and range from a
157 minimum of around 1 cm/hr in April to a maximum of 2.2 cm/h on September 7. The largest storm
158 surge events of 69.7 cm occurred on November 2 and on December 9. Other storm surges events
159 of around 50 cm occurred over the year (Fig. 3b). The corresponding moving average for observed
160 sea water level range from a maximum of 31 cm in October to a minimum of -35 cm in November.
161 Four temporal windows are selected to better analyze the most important features of the dataset.
162 (Fig. 4,5).

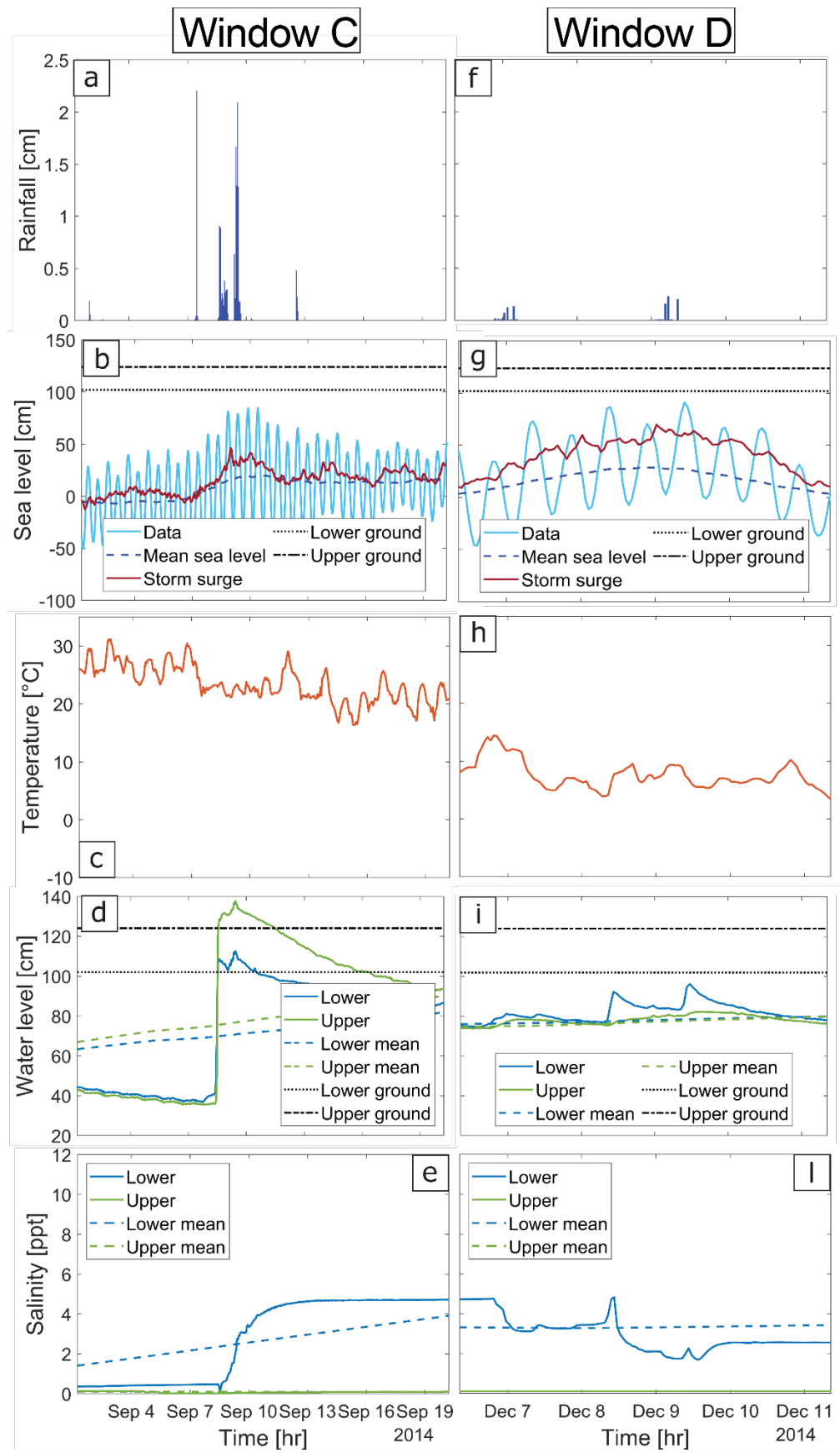


164 *Figure 3: a) Hourly precipitation at Hog Island station; b) observed tidal data with moving average and storm*
165 *surges at Kiptopeke station (NOAA); c) hourly temperature at Hog Island station; d) groundwater level in the lower*
166 *and the upper wells, corresponding moving averages and ground surface; e) salinity in the lower and upper wells*
167 *with corresponding moving averages. Yellow stars in b) identify the most significant storm surges.*



169 Figure 4: Temporal windows with measured hydrological variables. Windows A from 10 February 2014 at 8.30 am
170 to 15 February at 8.30 am, Windows B from 1 July 2014 at 1.30 am to 15 July at 1.30 am. a) Rainfall events; b)
171 observed tidal data, moving average of observed tidal data, storm surge; c) hourly temperature at Hog Island station;
172 d) groundwater level in the lower and upper wells, corresponding moving averages and ground surface; e) salinity
173 in the lower and upper wells with corresponding moving averages. Note that: to better illustrate the data in *the*

windows, the horizontal axes have different time interval.



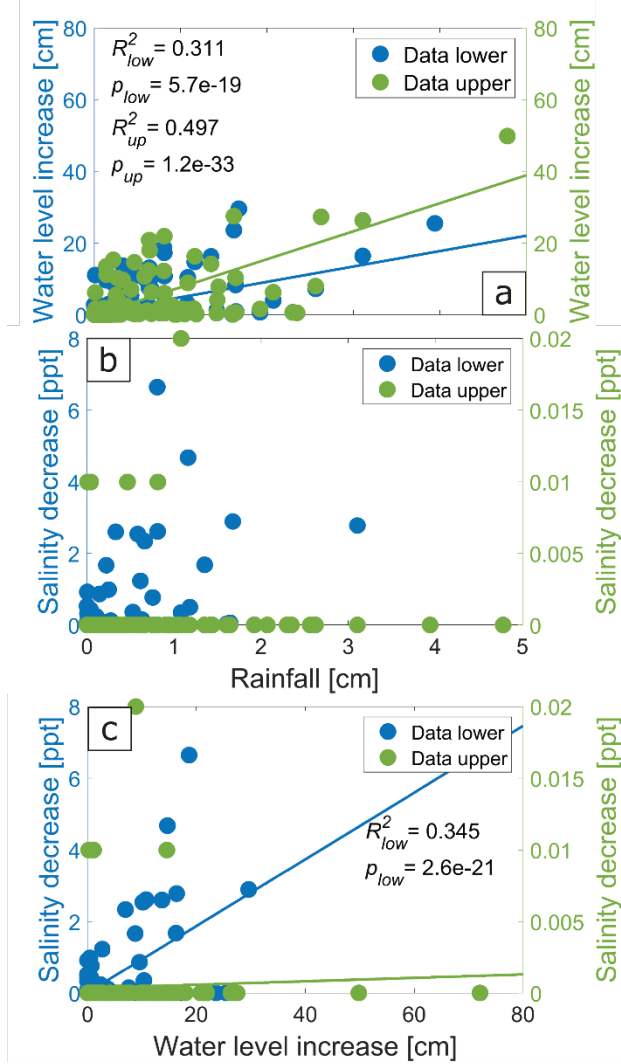
176 *Figure 5: Temporal windows with measured hydrological variables. Windows C from 1 September 2014 at 5.30 am*
177 *to 20 September at 5.30 am and Windows D from 6 December 2014 from 8.30 am to 11 December at 8.30 am. a)*
178 *Rainfall events; b) observed tidal data, moving average of observed tidal data, storm surge; c) hourly temperature*
179 *at Hog Island station; d) groundwater level in the lower and in the upper wells, corresponding moving averages*
180 *and ground surface; e) salinity data in the lower and upper wells with corresponding moving averages. Note that:*
181 *to better illustrate the data in the windows, the horizontal axes have different time interval.*

182

183 **3.1 Precipitation and groundwater levels**

184 In general, precipitation events are reflected in the groundwater level dataset as instantaneous
185 increases (Fig. 6a). Cumulative rainfall is calculated for each precipitation event, neglecting the
186 rainfall that moved as runoff when the soil was fully saturated. In both wells groundwater level
187 significantly increases ($R^2=0.311$ $p<0.05$ in the lower well and $R^2=0.497$ $p<0.05$ in the upper well)
188 as the rainfall amount increases. A consistent increase in water level from few centimeters to
189 around 40 cm occurs when rainfall amounts are above 1 cm. From September 7 to September 9
190 precipitation events between 3 and 8 cm along with storm surges between 10 and 40 cm cause a
191 water level increase of around 70 cm in the lower well and of around 100 cm in the upper well,
192 exceeding the ground surface respectively of 10.6 cm and of 13.8 cm (Fig. 5d). A precipitation
193 event of 2.62 cm occurred between February 12 and February 13, and it is reflected as an increase
194 of 22 cm in the lower well and of 27.30 cm in the upper well (Fig. 4a,d). This event floods the
195 ground surface at the lower location with 3.3 cm. A precipitation event of around 1 cm causes a
196 groundwater increase of 3 cm in Window D (Fig. 5f,i). In Window B (Fig. 4f,1), a similar
197 precipitation events cause groundwater increases between 5 cm and 12 cm. Therefore,
198 groundwater level response to precipitation is not always the same. This can be explained by the
199 presence of lateral water fluxes affecting the water table elevation and antecedent soil moisture
200 conditions. Some precipitation events in Windows A (Fig. 4a,d), C (Fig. 5a,d) and D (Fig. 5f,i) are
201 not reflected in the groundwater level. This discrepancy might be due to the location of the weather

202 station, which is several kilometers away. After each precipitation event, water level tends to
 203 decrease due to hydrologic recession dynamics.



204

205 *Figure 6: a) Groundwater level increments associated to cumulative rainfall amounts. Salinity drops associated to:*
 206 *b) cumulative rainfall amounts and c) ground water level increments. Salinity decreases on vertical axis are*
 207 *expressed as absolute values.*

208 3.2 Evaporation and groundwater levels

209 According to Gardner et al. (2002), evapotranspiration triggers a daily step-like decrease in the
 210 elevation of the groundwater table. This typical trend can be seen during the warmer summer
 211 season, for example, in window B (Fig. 4i). During sunlight hours, evapotranspiration is higher,

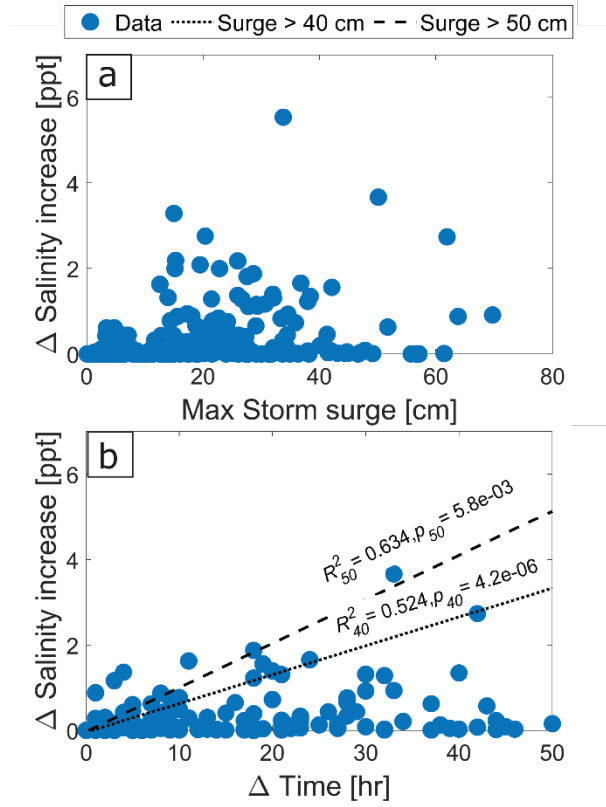
212 due to the combined effects of vegetation transpiration and soil evaporation; the higher the external
213 air temperature the higher the decrease in groundwater level. The groundwater level in both wells
214 remains quite constant during the nighttime hours. The daylight decrease is between 3 cm and 4
215 cm. An overall drop of 30 cm can be reached in this period, if the instantaneous increments due to
216 precipitation are not strong enough to increase the average groundwater level (Fig. 4i). The
217 evapotranspiration effect is reduced in the fall season. In window C (Fig. 5d), the groundwater
218 level drops only 1 cm during the daylight hours. The step-like decrease associated to
219 evapotranspiration is not present during the winter season.

220 **3.3 Salinity**

221 In the upper well, salinity is around zero and not related to precipitation events (Fig. 6b). Here,
222 groundwater can be considered freshwater (Fig. 3e). In the lower well, the salinity trend is strictly
223 connected to lateral fluxes of water. Precipitation events are reflected in the salinity record as
224 instantaneous drops due to dilution effects of the additional rainfall water. The decrease in salinity
225 is not correlated to rainfall amount (Fig. 6b). In Window A and Window B (Fig. 4a,e,f,l) two similar
226 rainfall amounts (2.62 cm and 2.35 cm) cause very different decreases in salinity (6.64 ppt and
227 0.20 ppt respectively). The second precipitation event in Window C (Fig. 5a,e), is not felt in the
228 salinity record. Instantaneous drops in salinity are instead correlated to water level ($R^2=0.345$
229 $p<0.05$, Fig. 6c). Once again, the salinity drops are related to water level increases calculated
230 neglecting runoff effects. In particular, when water level increases from 0 cm to 15 cm, the absolute
231 value of salinity drops increase linearly from 0 ppt to 3 ppt. The highest values of 6.64 ppt in terms
232 of salinity drop is reached during the precipitation event on 12 February (Fig. 4e). After each
233 precipitation event, salinity value increases fast, tending to reach the value before rainfall dilution,
234 and sometimes surpassing it.

235 In Window A, C, and D the salinity increase after storms seems to be associated to surge events.
236 In Window A (Fig. 4b,e), a storm surge event of 51.7 cm increased the salinity of 1.69 ppt
237 compared to the value before the storm, while in window C (Fig. 5b,e) a storm surge event of 45.9
238 cm slowly increased the salinity of 4.55 ppt. After this increase the salinity level remains higher.
239 A storm surge event of 69.7 cm, occurred on December 8, increases the groundwater level and
240 salinity respectively of 20 cm and 1.67 ppt in the lower well (Fig. 5i-l). This event leads
241 groundwater level in the lower well to reach level higher than in the upper well, inverting the
242 groundwater flux (negative hydraulic gradient). Rainfall events are not detected over this time.
243 Salinity increases when storm surge occurs, but the variables are not significantly correlated (Fig.
244 7a). Storm surge effects on salinity are tested considering maximum storm surges and their time
245 duration, when no precipitation events occur (Fig. 7b). A significant correlation is found between
246 storm surge duration and salinity increase for storm surge events higher than 40 cm (Fig. 7b).
247 In Window B (Fig. 4l) we detect a diurnal salinity oscillation due to evapotranspiration in a time
248 period not affected by precipitation events. During sunlight hours, when evapotranspiration is
249 higher and water level is decreasing, salinity tends to decrease, while during the nighttime when
250 evapotranspiration is low and groundwater levels are constant salinity tends to increase. Moreover,
251 in this time window neap-spring tidal modulation seems to affect variations in salinity. During the
252 neap tide the average salinity is around 3 ppt while during the spring tide the salinity is around 4
253 ppt.

254



255

256 *Figure 7: a) Salinity increments associated to maximum storm surge events and b) to storm surge duration in the*
 257 *lower well. Positive correlation between time duration and salinity increases for storm surge higher than 40 cm is*
 258 *shown.*

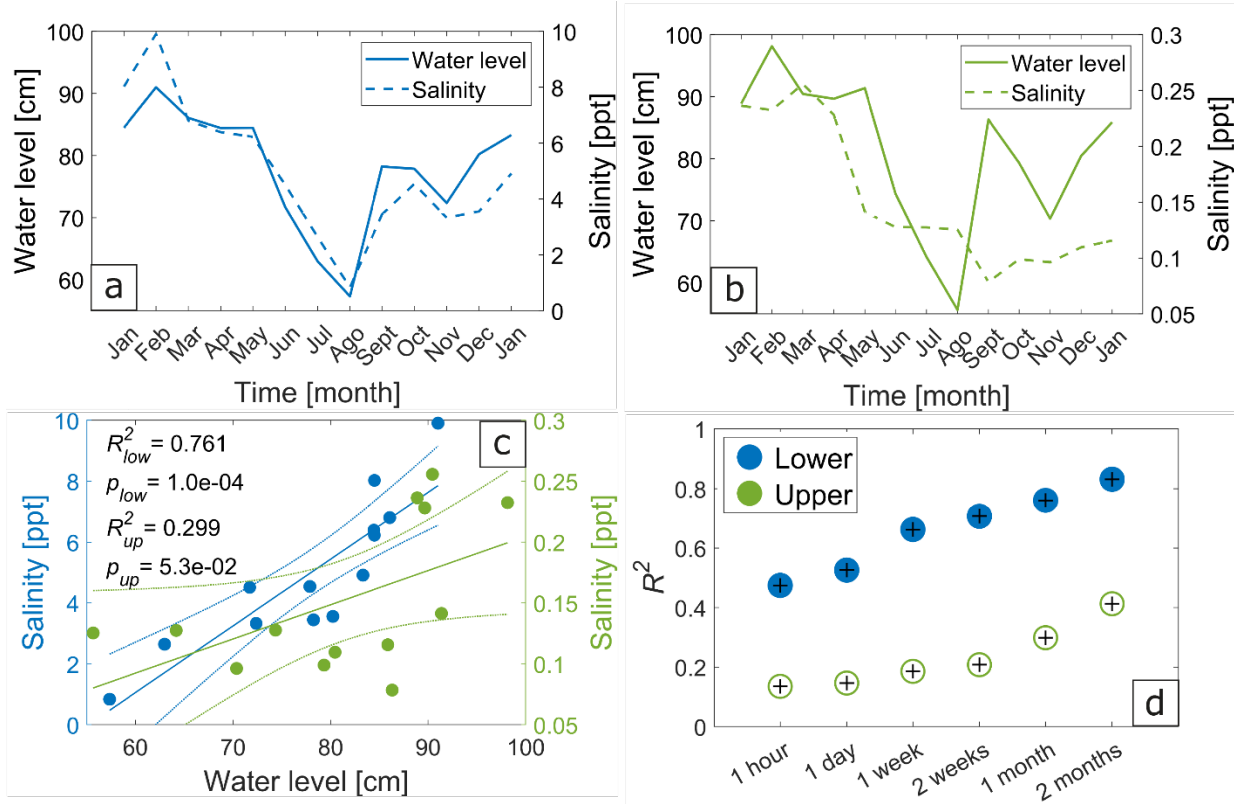
259 **3.4 Weekly and monthly relationships among groundwater level, groundwater salinity,
 260 evapotranspiration, sea level and rainfall.**

261 The relationships between groundwater level, salinity, rainfall, seawater level and
 262 evapotranspiration are analyzed using a linear regression analysis. The variables are correlated
 263 considering a temporal window spanning from 1 hour to 2 months. All variables are averaged
 264 across the temporal windows. Monthly salinity is significantly correlated to monthly groundwater
 265 level in the lower well (Fig. 8a). The correlation is also significantly positive for all temporal
 266 windows, with R^2 values ranging from 0.475 to 0.832 (Fig. 8d). The relationships between
 267 groundwater level, and rainfall, temperature, upstream and downstream hydraulic gradients are
 268 presented in Fig. 9, 10 and 11. The hydraulic gradients are considered here as a proxy for the flux

269 of water reaching the lower well from upstream or discharging toward the marsh. Monthly
270 groundwater levels are significantly correlated to temperature, upstream discharge from the upper
271 well and downstream discharge to sea (Fig. 9). A significant negative correlation is present
272 between groundwater level and temperature with a R^2 ranging from 0.336 for a one-week window
273 to 0.533 for a one-month window on a yearly scale (Fig. 11a). Therefore, upstream hydraulic
274 gradient has the strongest control on groundwater level, while rainfall is weakly correlated to
275 groundwater levels. On a seasonal scale, correlation between groundwater level and upstream
276 hydraulic gradient is always significantly positive for all seasons with R^2 values higher than 0.385
277 (Fig. 11 b,c,d,e). The temperature effect is significant during summer (Fig. 11 c) reaching R^2 values
278 of 0.771 for a two-week window. Groundwater level is significantly correlated to downstream
279 discharge in spring and summer with R^2 values higher than 0.331, for one-day and one-month
280 temporal windows (Fig. 11 b,c).

281 In Figure 11 we report the determination coefficients between salinity, rainfall, temperature,
282 upstream and downstream hydraulic gradients (Fig. 11 f, g, h, i, l). Monthly groundwater salinity
283 is significantly correlated to temperature, upstream discharge from the upper well and downstream
284 discharge to the marsh (Fig. 10). The correlation between salinity and hydraulic gradients is
285 significantly positive with R^2 values higher than 0.315 for temporal windows ranging from 1 day
286 to 1 month on a yearly scale (Fig. 11f). Salinity is negative correlated to temperature with R^2 values
287 ranging from 0.341 to 0.461 for temporal windows from 1 hour to 1 month (Fig. 11f) on a yearly
288 scale. Salinity and upstream hydraulic gradient are significantly correlated in summer and fall (Fig.
289 11 h,i). Downstream hydraulic gradient has the most remarkable effect on salinity during spring
290 and summer (Fig. 11 g, h). Temperature variations are significantly felt in the salinity trend during
291 winter and fall season (Fig. 11 i, l).

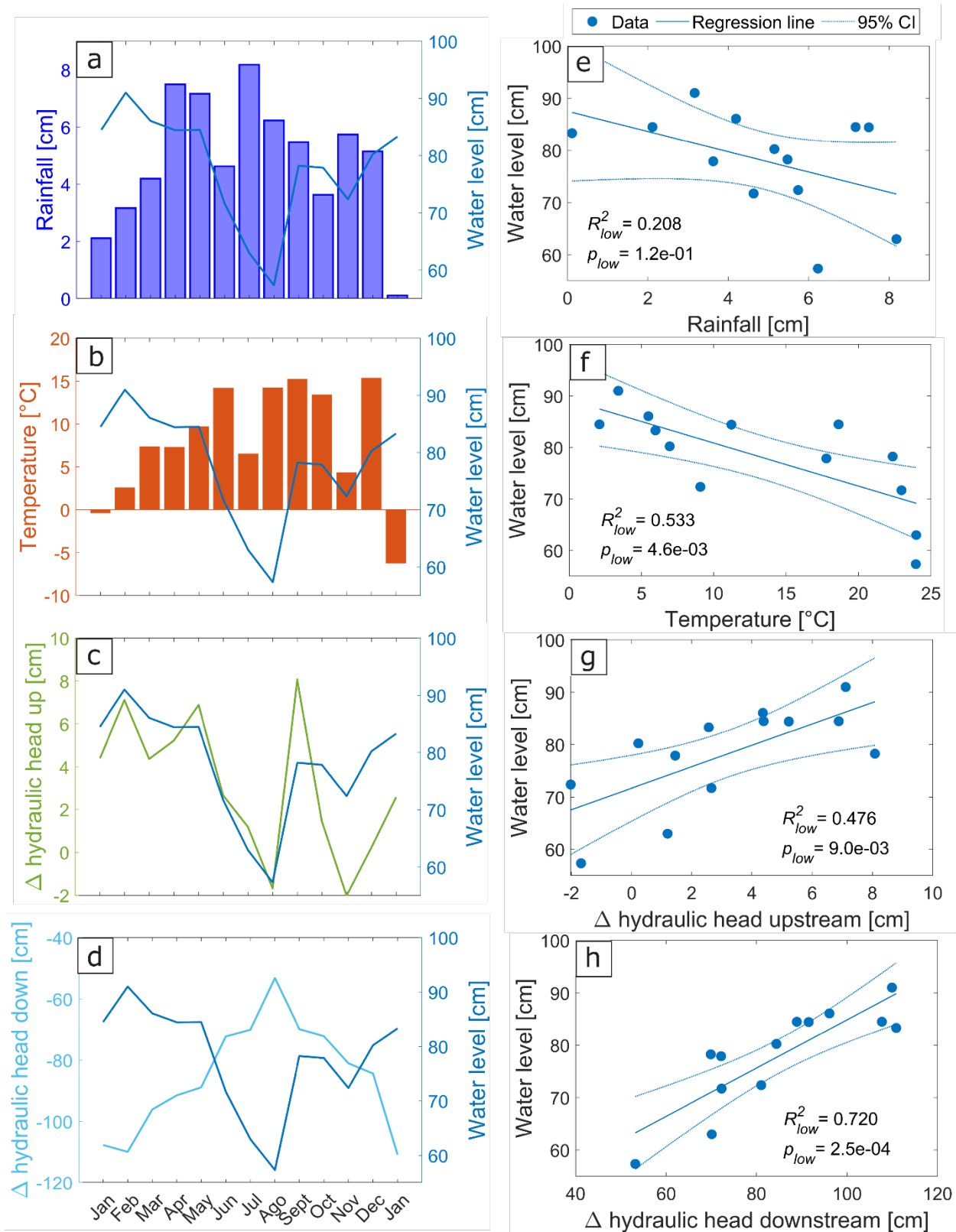
292 A multiple regression analysis is conducted considering only independent variables leading to
293 significant effects on the dependent variables of groundwater level and salinity on a yearly scale
294 (Table 1, 2). Groundwater level is correlated to temperature, upstream and downstream hydraulic
295 gradients while groundwater salinity is correlated to groundwater level, upstream and downstream
296 gradients and temperature. A first model considering all variables is proposed to describe
297 groundwater level and salinity trends (Table. 1, 2). Multicollinearity leads to non-significant
298 coefficients for some independent variables even if the regression as a whole is significant.
299 Redundant information is provided by different variables. After looking for the best combinations
300 among variables, two other models are proposed. Both salinity and groundwater level are analyzed
301 in a multivariate space firstly with upstream and downstream hydraulic gradients, and then with
302 upstream hydraulic gradients and temperature. For each temporal window adjusted R^2 values
303 increase in comparison to single regressions. Analysis of residuals confirm that removing one or
304 more variables from the multivariate dataset leads to information lost, and that the model well
305 represents the groundwater level trend. Parameters obtained in the sub-models are significant
306 ($p < 0.05$) and give a positive effect on the analysis.



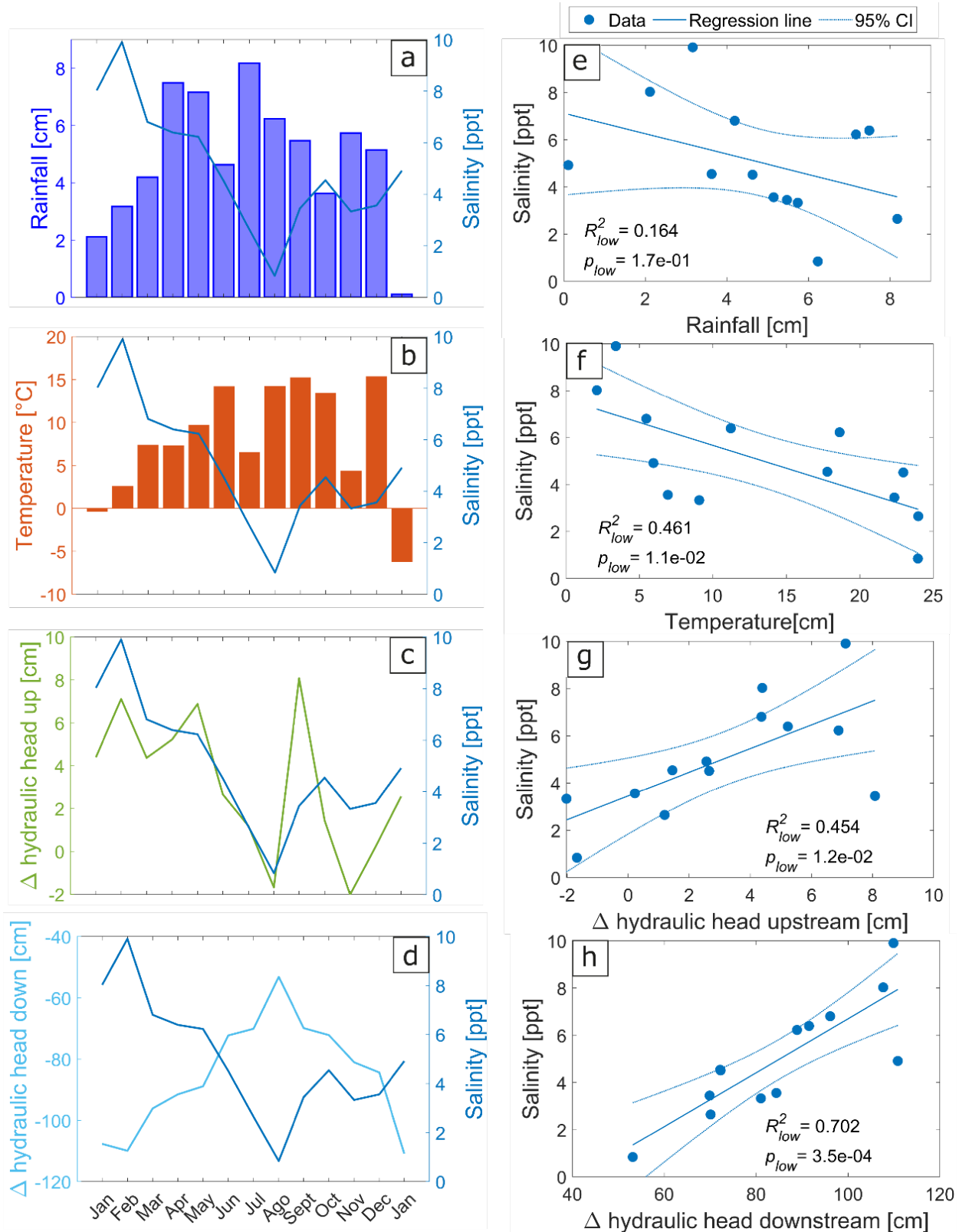
307

308

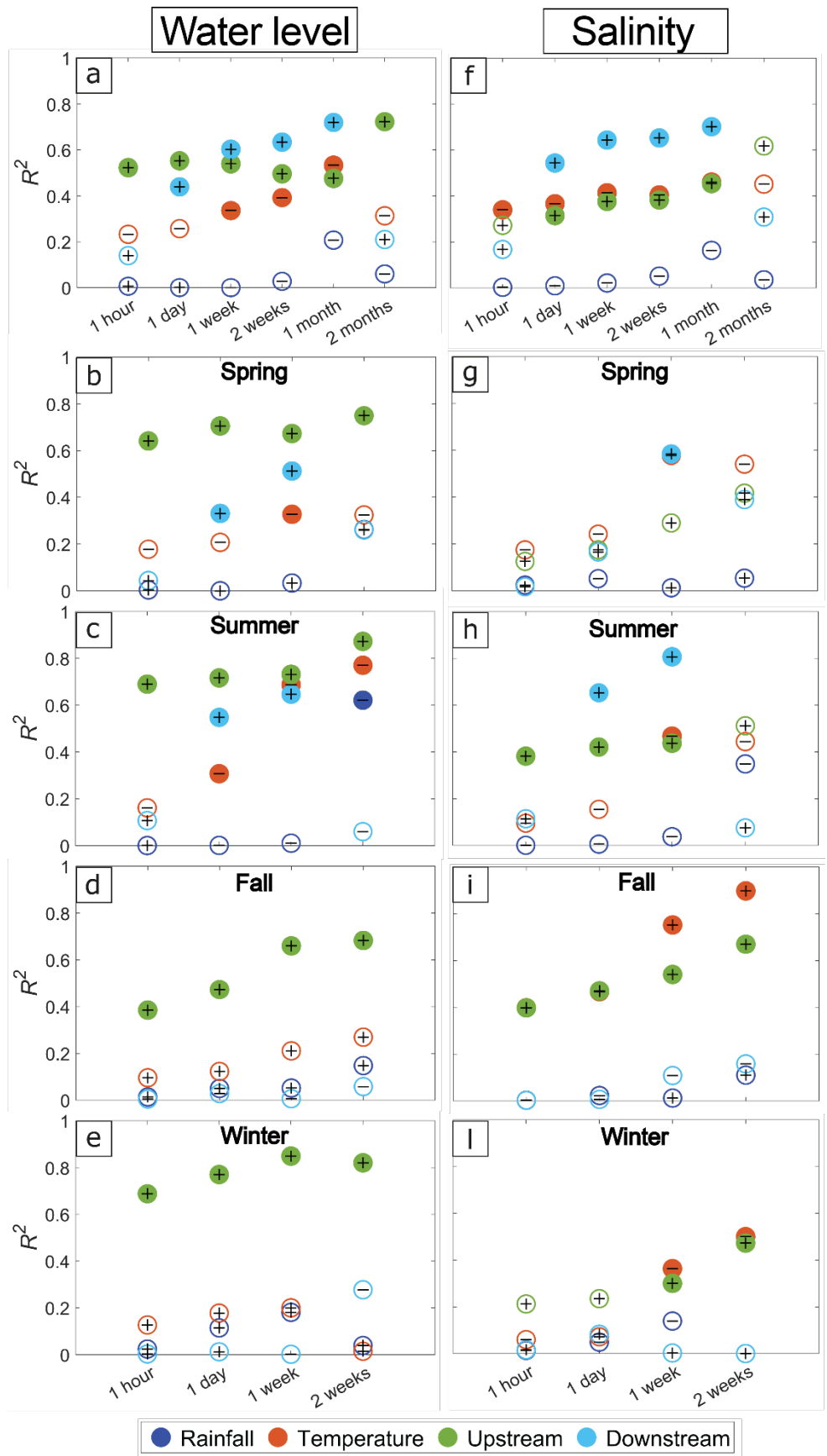
309 *Figure 8: Monthly groundwater level and salinity in a) lower well and b) upper well. c) Linear regression results for*
 310 *monthly groundwater levels and salinity; d) R^2 values for different temporal windows from 1 hour to 2 months over*
 311 *the year. Filled circles represent significant R^2 ($p < 0.05$), empty circles are not significant. The sign inside the circles*
 312 *indicates whether the correlation is positive or negative.*



315 *Figure 9: a) Monthly cumulative rainfall; b) average temperature; c) averaged upstream hydraulic gradient; and d)*
316 *averaged downstream hydraulic gradient related to monthly averaged groundwater levels. Linear regression*
317 *analysis on monthly data are reported in e), f), g), h).*



320 *Figure 10: a) Monthly cumulative rainfall; b) averaged temperature; c) averaged upstream hydraulic gradient;*
321 *and d) averaged downstream hydraulic gradient related to monthly averaged groundwater salinity. Linear*
322 *regression analysis on monthly data are represented in e), f), g), h).*



324

325 *Figure 11: Linear regression analysis for groundwater level (a, b, c, d, e) and salinity (f, g, h, i, l) as a function of*
 326 *rainfall, temperature, upstream and downstream hydraulic gradients for different temporal windows. a), f) from 1*
 327 *hour to 2 months over the year. From 1 hour to 2 weeks over spring b), g), summer c), h) fall d), i) and winter d), l).*
 328 *Empty circles represent not significant $R^2(p>0.05)$. The sign inside the circles indicates whether the correlation is*
 329 *positive or negative.*

330

331 *Table 1: Multiple regression analysis results. Groundwater level is correlated to upstream hydraulic*
 332 *gradient, downstream hydraulic gradient and temperature.*

h = water level, Δh_{up} = upstream discharge, Δh_{low} = downstream discharge, t = temperature				
$*P$ -value >0.05 , $*P$ -value <0.05 , $**P$ -value <0.01 , $***P$ -value <0.001				
Dependent variable	Independent variable	Time window	Model coefficients	Adjusted R^2
Groundwater level	• Upstream discharge • Downstream discharge • Temperature	1 hour	78.661(***)+1.881 Δh_{up} (***)+0.022 Δh_{low} (***)- 0.622 t (***)	0.714 (***)
		1 day	73.922(***)+1.898 Δh_{up} (***)+0.071 Δh_{low} (**)- 0.580 t (***)	0.761 (***)
		1 week	70.464(***)+1.823 Δh_{up} (***)+0.108 Δh_{low} (*)- 0.540 t (***)	0.806 (***)
		2 weeks	72.552(***)+1.750 Δh_{up} (***)+0.087 Δh_{low} (*)- 0.557 t (*)	0.806 (***)
		1 month	78.999(**)+1.734 Δh_{up} (**)+0.034 Δh_{low} (*)- 0.688 t	0.860 (***)
		2 months	55.010(*)+2.840 Δh_{up} (*)+0.183 Δh_{low} (*)-0.194 t (*)	0.886 ()
	• Upstream discharge • Downstream discharge	1 hour	65.555(***)+1.858 Δh_{up} (***)+0.074 Δh_{low} (***)	0.561 (***)
		1 day	51.246(***)+1.591 Δh_{up} (***)+0.257 Δh_{low} (***)	0.680 (***)
		1 week	44.707(***)+1.382 Δh_{up} (***)+0.342 Δh_{low} (***)	0.761 (***)
		2 weeks	44.057(***)+1.276 Δh_{up} (***)+0.352 Δh_{low} (***)	0.773 (***)
		1 month	43.271(***)+1.147 Δh_{up} (*)+0.366 Δh_{low} (***)	0.807 (***)
		2 months	45.421(**)+2.907 Δh_{up} (**)+0.260 Δh_{low} (*)	0.920 (**)
	• Upstream discharge • Temperature	1 hour	80.748(***)+1.919 Δh_{up} (***)-0.651 t (***)	0.711 (***)
		1 day	80.803(***)+2.033 Δh_{up} (***)-0.680 t (***)	0.757 (***)
		1 week	81.190(***)+2.039 Δh_{up} (***)-0.713 t (***)	0.802 (***)
		2 weeks	81.407(***)+1.911 Δh_{up} (***)-0.707 t (***)	0.810 (***)
		1 month	82.446(***)+1.797 Δh_{up} (*)-0.747 t (***)	0.874 (***)
		2 months	77.256(***)+2.694 Δh_{up} (**)-0.610 t (*)	0.905 (**)

333

334 *Table 2: Multiple regression analysis results. Groundwater salinity is correlated to groundwater level,*
 335 *upstream hydraulic gradient, downstream hydraulic gradient and temperature.*

336

337

h = water level, Δh_{up} = upstream discharge, Δh_{low} = downstream discharge, t = temperature $*P$ -value > 0.05, $*P$ -value < 0.05, $**P$ -value < 0.01, $***P$ -value < 0.001					
Dependent variable	Independent variable	Time window	Model coefficients	Adjusted R ²	
Groundwater salinity	<ul style="list-style-type: none"> Upstream discharge Downstream discharge Temperature Water level 	1 hour	$1.941(***)+0.046 h(***)+0.160 \Delta h_{up}(***)+0.008 \Delta h_{low}(***)-0.121 t(***)$	0.601 (***)	
		1 day	$0.156(*)+0.030 h(*)+0.160 \Delta h_{up}(***)+0.039 \Delta h_{low}(***)-0.093 t(***)$	0.682 (***)	
		1 week	$-1.278(*)+0.049 h(*)+0.185 \Delta h_{up}(*)+0.035 \Delta h_{low}(*)-0.083 t(*)$	0.741 (***)	
		2 weeks	$-4.977(*)+0.078 h(*)+0.147 \Delta h_{up}(*)+0.046 \Delta h_{low}(*)-0.033 t(*)$	0.732 (***)	
		1 month	$-2.527(*)+0.043 h(*)+0.277 \Delta h_{up}(*)+0.048 \Delta h_{low}(*)-0.058 t(*)$	0.745 (**)	
		2 months	$13.949(*)-0.188 h(*)+1.098 \Delta h_{up}(*)+0.053 \Delta h_{low}(*)-0.168 t(*)$	0.996 (*)	
	<ul style="list-style-type: none"> Upstream discharge Downstream discharge 	1 hour	$-2.411(***)+0.241 \Delta h_{up}(***)+0.021 \Delta h_{low}(***)$	0.353 (***)	
		1 day	$-1.916(***)+0.159 \Delta h_{up}(***)+0.076 \Delta h_{low}(***)$	0.603 (***)	
		1 week	$-3.009(**)+0.185 \Delta h_{up}(***)+0.088 \Delta h_{low}(***)$	0.698 (***)	
		2 weeks	$-3.241(**)+0.218 \Delta h_{up}(***)+0.089 \Delta h_{low}(***)$	0.718 (***)	
		1 month	$-3.645(*)+0.278 \Delta h_{up}(*)+0.091 \Delta h_{low}(***)$	0.775 (***)	
		2 months	$-2.938(*)+0.609 \Delta h_{up}(*)+0.070 \Delta h_{low}(*)$	0.912 (**)	
	<ul style="list-style-type: none"> Upstream discharge Temperature 	1 hour	$6.383(***)+0.262 \Delta h_{up}(***)-0.161 t(***)$	0.574 (***)	
		1 day	$6.391(***)+0.295 \Delta h_{up}(***)-0.168 t(***)$	0.632 (***)	
		1 week	$6.2543(***)+0.356 \Delta h_{up}(***)-0.175 t(***)$	0.719 (***)	
		2 weeks	$6.035(***)+0.381 \Delta h_{up}(***)-0.167 t(***)$	0.708 (***)	
		1 month	$5.948(***)+0.444 \Delta h_{up}(*)-0.173 t(***)$	0.773 (***)	
		2 months	$5.803(***)+0.550 \Delta h_{up}(*)-0.173 t(*)$	0.942 (**)	

338

339

340

4. Discussion

341 The data collected at the two wells shed light on the groundwater dynamics in the forested area of
 342 the Eastern Shore of Virginia National Wildlife Refuge in 2014. In particular, the four temporal
 343 windows and the correlation analysis among hydrological variables enable to draw important
 344 conclusions about the effects of external drivers on water table elevation and groundwater salinity,
 345 which in turn control vegetation cover.

346

4.1 Water Levels

347 Rainfall events, evapotranspiration, groundwater fluxes from the uphill and toward the marsh
348 control groundwater level in different ways across short and long temporal scales (Fig. 12a).
349 Rainfall causes instantaneous increases in the groundwater level. The larger is the cumulative
350 rainfall in a single event, the higher is the increment in groundwater level. This occurs at both
351 wells suggesting a significant positive correlation between the two variables at the event scale (Fig.
352 6a). After every water level peak due to rainfall, the water level values decrease, approaching the
353 mean water level, as consequence of the deep-water recharge process. Cumulative rainfall does
354 not have a direct effect on the groundwater level in the lower well on a long timescale (Fig. 9a,e
355 ,11a, b, c, d, R^2 values are not significant). The inter-storm periods are on average around 2 days
356 for all seasons (Fig. 3a). During spring and summer, the precipitation events are more intense, on
357 average around 0.4 cm, while during winter and fall precipitation is around 0.2 cm for each event.
358 The longer the inter-storm periods are, the more likely is the groundwater level to decrease. Under
359 the same inter-storm conditions, if the precipitation event is conspicuous, ponding and surface
360 runoff will likely occur (Assouline et al. 2007). During summer, mainly in July and August,
361 precipitation is abundant, but the water level is decreasing due to evapotranspiration.
362 In the four temporal windows, it is possible to see how in correspondence of particular precipitation
363 events, groundwater levels reach values higher than the ground surface at both wells. This happens
364 in window A (Fig. 4d) and C (Fig. 5d) in the lower well, and in windows C in the upper well (Fig.
365 5d). During these events the soil can be considered saturated, and water in excess accumulates
366 over the ground level in correspondence of the wells. Additional water might flow along the slope
367 as runoff. According to the data reported in the four windows, it takes between 7 hours (Fig. 4d)
368 to 2 days (Fig. 5d) to terminate water ponding and resume water infiltration, depending on quantity
369 and frequency of external precipitation inputs.

370 Flooding events are dangerous for *Pinus taeda* survival. Reduced oxygen availability and a
371 significant decrease in soil redox potential directly affect water uptake from the soil (Anderson
372 and Pezeshki, 1999, Pezeshki 1991). Intermittent flooding can cause different results on stomatal
373 conductance and net photosynthetic activity in seedling of different species, reaching the worst
374 scenario when the reduction is so large that plants cannot recover any more (Anderson and
375 Pezeshki, 1999). Pezeshki, (1991) indicates that a reduction in soil redox potential of 100 mV
376 occurs in less than 10 days of flooding. Over a treatment period of 30 days, flooding resulted in a
377 substantial reduction of soil redox potential, stomatal conductance and biomass (Pezeshki, 1991).

378 Evapotranspiration is one of the most significant drivers of groundwater level at longer temporal
379 scales. Evapotranspiration mostly occurs during summer (Fig. 4i) when air temperature in the
380 daylight hours is high and photosynthesis takes place. During this period, trees, fully foliated,
381 transpire to maintain their inner temperature. This results in a decrease of mean water level of
382 about 30 cm in both wells over the summer period. Evapotranspiration dominates over the other
383 hydrological fluxes. The role of evapotranspiration is confirmed in the single regression analysis
384 for the lower well (Fig. 11a, b, c, d, e). Over the year, the maximum correlation between
385 groundwater level and temperature is reached on a temporal window of one month (Fig. 9b, 11a).

386 The hydraulic gradient between the lower well and sea level is the other chief variable controlling
387 groundwater levels. The higher is the groundwater level, the more abundant is the downhill flux
388 of water (Fig. 11a). During spring and summer, the groundwater level is positively correlated to
389 discharge toward the marsh (Fig. 11b, c). This suggests that low groundwater levels are more
390 affected by the discharge to the marsh. During winter and fall, high groundwater levels are not
391 significantly affected by the discharge to the marsh. The existence of groundwater discharge to the
392 sea has been already investigated in coastal regions (Li, 1999; Werner, 2013; Robinson, 2006;

393 Taniguchi 2002, Michael et al. 2005). Both fresh and salt groundwater discharges are present. The
394 saline flow involves the deeper zone, while the fresh groundwater flow moves closer to the ground.
395 On the basis of our analysis we can suppose the presence of a fresh groundwater flow to the marsh
396 affecting the groundwater level at our site.

397 Storm surges are not significantly correlated to increments in groundwater level. Although in
398 windows A, C and D (Fig. 4b, d, 5b, d, g, i) storm surge events do increase mean groundwater
399 values. The storm surge events occur in correspondence to significant rainfalls that usually saturate
400 the soil (Fig. 4a, Fig. 5a,f). They do not lead to an instantaneous change in water level, but they
401 likely magnify the water level increase. Note that during the study period there was not a major
402 storm surge able to flood the entire forest.

403 The hydraulic gradient from uphill to the lower well significantly affects groundwater levels. Over
404 the year the correlation between the two variables is significantly positive, reaching R^2 values
405 higher than 0.4 (Fig. 11a). The homogenous and sandy soil justifies this relation, favoring
406 groundwater flow downhill. A multiple regression analysis yields adjusted R^2 values higher than
407 0.56 considering a model where upstream and downstream hydraulic gradients are dependent
408 variables, and higher than 0.71 considering a model where upstream hydraulic discharge and
409 temperature are dependent variables. An analysis on their correlation confirm they are negative
410 linked. A model considering all dependent variables suggest that temperature and downstream
411 discharge carry a redundant information, making multiple regression parameters not significant.
412 (Table 1). Overall, the multiple regression provides better results in comparison to single
413 regression.

414 **4.2 Salinity**

415 Groundwater salinity is not significantly correlated to precipitation events, even if it is possible to
416 recognize an instantaneous decrease in salinity as the rainfall amount increases (Fig. 6b). As soon
417 as the rainfall stops the salinity increases to values similar to the pre-event conditions.

418 As temperature increases, evapotranspiration increases and salinity decreases (Fig. 11). During fall
419 the correlation between salinity and temperature is significantly positive (Fig. 11i). In September,
420 an intense rainfall event occurred along with a large storm surge, and groundwater levels increased
421 until reaching the soil (Fig. 3a, b, d, 5a, b, d). A water table near the surface leads to higher
422 evaporation. When this occurs, salt ions are likely to accumulate near the ground surface, moving
423 upwards along with water in the unsaturated zone and leaving the original depth (Mohamed, 2000).
424 This could justify lower salinity values collected by CTD at a fixed deeper position.

425 The groundwater flux to the sea is positively correlated to salinity in the lower well (Fig. 11f). This
426 occurs mainly during spring and summer (Fig. 11g, h). A net freshwater discharge can justify this
427 trend. When groundwater is high in the lower well, water from the top fresh layer flows toward
428 the marsh, and it is replenished by saltier water coming from below (Fig. 12b). A release of
429 freshwater from the ground decreases the dilution of salt water, and salinity increases. The
430 maximum increase of salinity is reached in September when sea level was around 85 cm on
431 NADV88 (Fig. 6b). In that month, a significant storm surge event (Fig. 5b) acted along with high
432 temperatures and groundwater discharge from uphill to increase salinity. The conspicuous amount
433 of rainfall that occurred during the storm was unable to infiltrate the saturated soil, and moved
434 away as runoff. A similar event occurred in Window A (Fig. 4b). In this period, most of the rainfall
435 infiltrated. A storm surge occurred after some hours from the rainfall event. Salinity first rapidly
436 decreased as a consequence of rainfall, and then increased because of mixing with the saline water.
437 Salinity kept increasing until it surpassed the value before the event due to storm surge effects.

438 Storm surge events can be recognized as a slow increase in salinity in comparison to the steep
439 increase after rainfall dilution. When no precipitation events occur, salinity increases are positively
440 correlated to storm surge duration, if storm surges are higher than 40 cm (Fig. 7b).

441 The hydraulic gradient between the upper and lower well is positively correlated to salinity over
442 the year and in each season (Fig. 11f, g, h, i, l). Therefore, a large groundwater discharge from
443 uphill augments groundwater salinity. We suppose that the discharge from uphill becomes more
444 saline during its infiltration path, reaching deeper saline areas, and recharging the lower well from
445 below.

446 Groundwater salinity is strongly correlated to groundwater level in the lower well, for all temporal
447 windows ranging from 1 hour to 2 months (Fig. 8a, c, d). As the groundwater level increases, the
448 salinity increases and vice versa. The groundwater level is directly linked to the recharge from
449 uphill, the discharge toward the marsh, and evapotranspiration.

450 A multiple regression analysis yields adjusted R^2 values higher than 0.35 considering a model
451 where upstream and downstream hydraulic gradients are independent variables, and higher than
452 0.57 considering a model where upstream hydraulic discharge and temperature are independent
453 variables. A model considering all independent variables suggest that groundwater level,
454 temperature and downstream discharge carry redundant information, making multiple regression
455 parameters not significant (Table 2). The models proposed are those leading to the best results in
456 terms of significance as a whole and for each parameter. Overall, the multiple regression provides
457 better results in comparison to single regressions.

458 We put forward the hypothesis that the discharge toward the marsh and evapotranspiration are
459 depleting the surficial freshwater layer, while the uphill groundwater flux brings saltier water. An

460 increase in water table elevation would therefore expose the freshwater layer to more
461 evapotranspiration and fluxes to the marsh, reducing salinity. When the water table is low, more
462 freshwater can be safely stored in the ground and in the root zone.

463 The sharp geotechnical boundary between forest and the marsh can also accentuate these
464 dynamics. The impermeable marsh soils rich in silt and clay might prevent deep groundwater
465 fluxes, forcing the water to move superficially from the forest to the marsh as return flow or runoff
466 (Fig. 12b). This surficial flux would deplete the freshwater stored in shallow layers, increasing
467 salinity. In the sandy hillslope, water from uphill can infiltrate and move in deeper layers, mixing
468 with saltier water and thus bringing salt to the downhill location. Our results indicate that higher
469 groundwater levels would trigger evapotranspiration and fluxes to the marsh, removing freshwater
470 and increasing salinity at the roots depth. This negative effect can be magnified by sea level rise,
471 which would further increase the water table elevation, and deplete freshwater in the roots area,
472 encouraging salt water intrusion from deeper layers on long timescale.

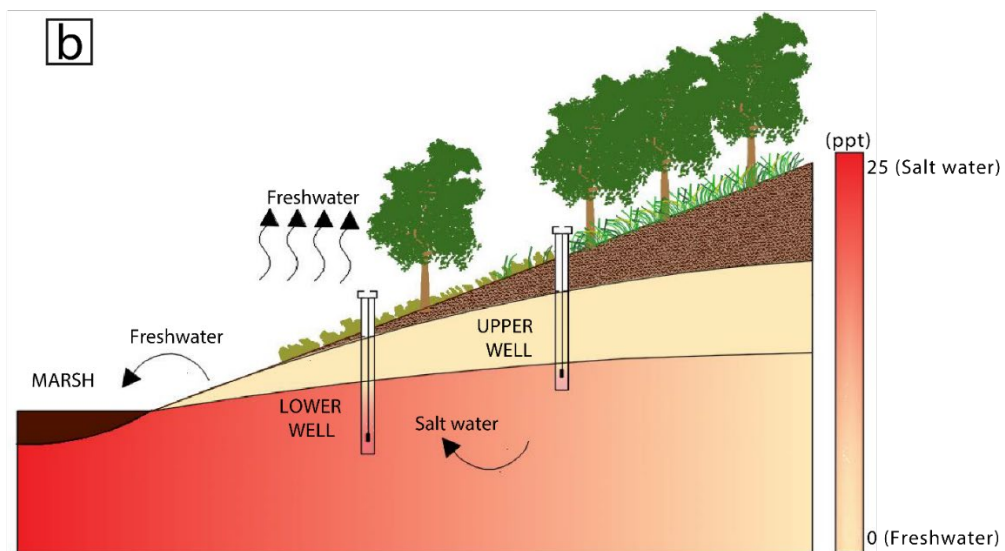
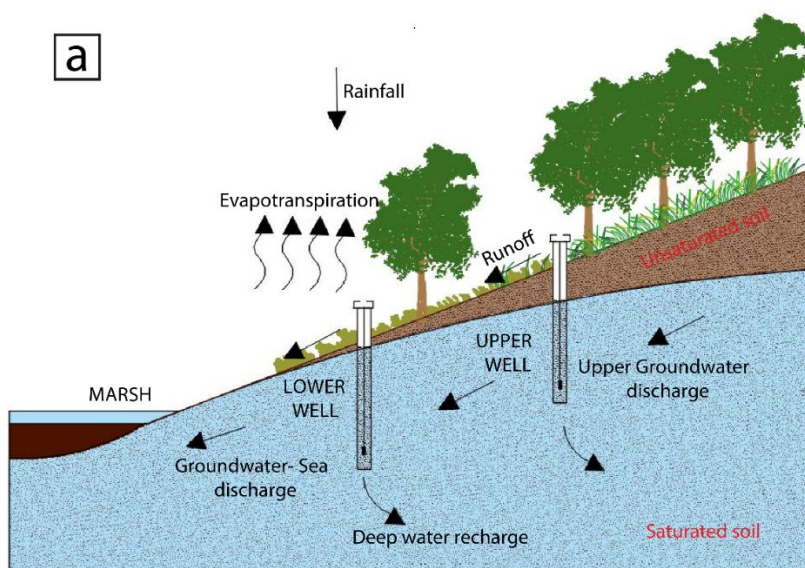
473 The maximum correlation among all variables is reached using monthly averages, we therefore
474 conclude that drivers of groundwater hydrology act at temporal scale of weeks and not
475 instantaneously. For example, the average sea level in a month has more effect on the water table
476 elevation than the instantaneous water level.

477 Sandy soils can faster drain water infiltrating from the unsaturated zone to recharge the
478 groundwater systems (Kutilek and Nielsen 1994). In clay soils, water movement is slower and the
479 effect of rainfall inputs on groundwater level is likely felt in a weaker way (Cao et al. 2012). In
480 low-lying areas, dominated by shallow water, an upward discharge from below tend to pond the
481 ground surface. In clay soils the evaporation rate is higher, and water tends to pond easily (Kutilek
482 and Nielsen 1994). Moreover, sandy soils are less prone to salinization than clay soils because

483 salts attach to small particles while they are easily leached in sand. When flow is faster (high
484 hydraulic conductivity), advection dominates (Batany et al. 2019), so that groundwater flow from
485 the upper to the lower sites can bring salts leached in deeper zones.

486 Plants that tolerate osmotic stress can adapt to new salinity conditions. These plants exclude Na^+
487 from leaf blades and roots or compartmentalize Na^+ and Cl^- at the cellular and intracellular level
488 (Munns and Tester, 2008). The latter method is less efficient because the accumulation space is
489 limited (Hasegawa, 2000). *Pinus taeda* is unable to use one of these approaches (Pezeshki, 1991),
490 and salt water disturbs its roots environment undermining photosynthetic activity (Nawaz, 2010).

491 In the lower zone of the forest, new salt-tolerant plant species can encroach where *Pinus taeda*
492 trees die because of salinization, ultimately expanding the marsh environment. First, invasive
493 species like *Phragmites australis* (Chambers et al. 1999) tend to expand finding better light
494 condition in the gaps of the dying forest. This species can tolerate low salinities (~ 5 ppt) (Lissner
495 et al. 1997; Hellings et al. 1992) but can be soon replaced by extremely salt-tolerant marsh species
496 like *Spartina patens*, *Juncus gerardi* and *Spartina alterniflora*, very common in the lower area of
497 Chesapeake Bay (Rice et al. 2000; Hester et al. 2001). In the regenerative zone, we did not detect
498 a significant increase in salinity. Here freshwater enables the forest to regenerate with saplings.



499

500 *Figure 12: a) Hydrological processes affecting groundwater levels at the forest boundary. b) chief hydrological*
 501 *fluxes affecting groundwater salinity at the roots elevation. The color indicates salinity levels*

502

503

504 **5. Implications for sea-level rise and coastal forests**

505 Our results can provide critical insight on the effect of sea level rise on coastal forests. Our data
 506 indicate that an increase in groundwater levels at the marsh boundary might trigger an increase in

507 salinity in the root zone. Sea level rise is likely to increase water levels in coastal aquifers; in some
508 coastal locations the percentage of flooded area by groundwater has already expanded due to
509 climate change (Rotzoll and Fletcher 2012). The percentage could be higher in topography-limited
510 systems like North Atlantic coast (Gleeson et al. 2011), where sea level rise is accelerating (Church
511 et al. 2006; Sallenger et al. 2012). This increase in groundwater levels will likely trigger an increase
512 in salinity. Similar results were presented by Michael et al. (2013) using numerical simulations. In
513 low-lying areas where groundwater recharge is topographically limited, an increase in sea level
514 results in the intersection of the groundwater table with the ground surface, favoring runoff and
515 reducing the amount of freshwater that can be stored in the soil. As a result, the freshwater
516 hydraulic head landward cannot balance SLR seaward, causing salinization of the aquifer.
517 Moreover, Michael et al. (2013) simulations show that the salinization rate is higher in isotropic
518 soils with high permeability, like those present at our study site. Our measurements confirm this
519 hypothesis, and provide a quantitative relationship between water level and salinity that can be
520 used to forecast the effect of sea level rise on forest ecosystems.

521 **6. Conclusions**

522 High resolution hydrological measurements in a coastal forest bordering a salt marsh indicate that
523 the groundwater is fresh in the higher regenerative zone, where tree saplings are present, while it
524 is brackish in the lower persistence zone, where only mature trees survive. In the short term
525 (timescale of hours), groundwater levels significantly increase after a rainfall while salinity
526 decreases. Storm surges are felt in the salinity trend as slow increments, as compared to the
527 instantaneous steep decrease caused by rainfall and subsequent increase due to mixing with saline
528 water.

529 In the medium term (timescales of weeks and months), temperature (a proxy for
530 evapotranspiration), uphill and downhill hydraulic gradients (a proxy for lateral groundwater
531 fluxes) significantly influence groundwater levels and salinity. Statistical analysis suggests that
532 rainfall is not a direct driver of water level and salinity at the monthly timescale. Surprisingly,
533 salinity at the roots depth is high when the water table is high. We ascribe this counterintuitive
534 result to depletion of the top freshwater layer caused by surficial and sub-surficial fluxes to the
535 marsh and increased evapotranspiration when water levels are high. We hypothesize that the lost
536 freshwater is replaced by more saline water flowing at depth from uphill. Sea level rise, by
537 increasing the water table, could therefore augment the salinity of the groundwater at the roots
538 depth, triggering forest dieback.

539

540 **Acknowledgments**

541 This research was funded by the USA National Science Foundation awards 1832221 (VCR
542 LTER), 1637630 (PIE LTER), and 2012322 (CZN Coastal Critical Zone). We thank William S.
543 Kearney for help with the fieldwork and the Eastern Shore of Virginia National Wildlife Refuge
544 for logistical support.

545
546 **References**

- 547 • Allen, J. A., Conner, W. H., Goyer, R. A., Chambers, J. L., & Krauss, K. W. (1998). Freshwater forested
548 wetlands and global climate change. *Vulnerability of coastal wetlands in the Southeastern United States, A*
549 *Biological Science Report USGS/BRD/BSR, Hawaii*, 33-44.
- 550 • Amit, H., Lyakhovsky, V., Katz, A., Starinsky, A., & Burg, A. (2002). Interpretation of spring recession
551 curves. *Groundwater*, 40(5), 543-551.
- 552 • Anderson, P. H., & Pezeshki, S. R. (2000). The effects of intermittent flooding on seedlings of three forest
553 species. *Photosynthetica*, 37(4), 543-552.
- 554 • Assouline, S., Selker, J. S., & Parlange, J. Y. (2007). A simple accurate method to predict time of ponding
555 under variable intensity rainfall. *Water resources research*, 43(3).
- 556 • Batany, S., Peyneau, P. E., Lassabatère, L., Béchet, B., Faure, P., & Dangla, P. (2019). Interplay between
557 molecular diffusion and advection during solute transport in macroporous media. *Vadose Zone*
558 *Journal*, 18(1), 1-15.
- 559 • Bertness, M. D., & Ellison, A. M. (1987). Determinants of pattern in a New England salt marsh plant
560 community. *Ecological monographs*, 57(2), 129-147.
- 561 • Blott, S. J., & Pye, K. (2001). GRADISTAT: a grain size distribution and statistics package for the analysis
562 of unconsolidated sediments. *Earth surface processes and Landforms*, 26(11), 1237-1248.
- 563 • Bruand, A., Hartmann, C., & Lesturgez, G. (2005). Physical properties of tropical sandy soils: A large
564 range of behaviours. In *Management of Tropical Sandy Soils for Sustainable Agriculture. A holistic*
565 *approach for sustainable development of problem soils in the tropics*.
- 566 • Cao, W., Sun, G., McNulty, S. G., Chen, J., Noormets, A., Skaggs, R. W., & Amatya, D. M. (2006).
567 Evapotranspiration of a mid-rotation loblolly pine plantation and a recently harvested stands on the coastal
568 plain of North Carolina, USA. In *Hydrology and Management of Forested Wetlands, Proceedings of the*
569 *International Conference, April 8-12, 2006, New Bern, North Carolina* (p. 5). American Society of
570 Agricultural and Biological Engineers.
- 571 • Carter, E. S., White, S. M., & Wilson, A. M. (2008). Variation in groundwater salinity in a tidal salt marsh
572 basin, North Inlet Estuary, South Carolina. *Estuarine, coastal and shelf science*, 76(3), 543-552.
- 573 • Church, J. A., & White, N. J. (2006). A 20th century acceleration in global sea-level rise. *Geophysical*
574 *research letters*, 33(1).
- 575 • Davarzani, H., Smits, K., Tolene, R. M., & Illangasekare, T. (2014). Study of the effect of wind speed on
576 evaporation from soil through integrated modeling of the atmospheric boundary layer and shallow
577 subsurface. *Water resources research*, 50(1), 661-680.
- 578 • Del Pilar Alvarez, M., Carol, E., Hernández, M. A., & Bouza, P. J. (2015). Groundwater dynamic,
579 temperature and salinity response to the tide in Patagonian marshes: Observations on a coastal wetland in
580 San José Gulf, Argentina. *Journal of South American Earth Sciences*, 62, 1-11.
- 581 • Desantis, L. R., Bhotika, S., Williams, K., & Putz, F. E. (2007). Sea-level rise and drought interactions
582 accelerate forest decline on the Gulf Coast of Florida, USA. *Global Change Biology*, 13(11), 2349-2360.
- 583 • Domec, J. C., Sun, G., Noormets, A., Gavazzi, M. J., Treasure, E. A., Cohen, E., ... & King, J. S. (2012). A
584 comparison of three methods to estimate evapotranspiration in two contrasting loblolly pine plantations: age-
585 related changes in water use and drought sensitivity of evapotranspiration components. *Forest Science*, 58(5),
586 497-512.
- 587 • Eltahir, E. A., & Bras, R. L. (1996). Precipitation recycling. *Reviews of geophysics*, 34(3), 367-378.

588 • Fagherazzi, S., Anisfeld, S. C., Blum, L. K., Long, E. V., Feagin, R. A., Fernandes, A., ... & Williams, K.
589 (2019). Sea level rise and the dynamics of the marsh-upland boundary. *Frontiers in Environmental*
590 *Science*, 7, 25.

591 • Fagherazzi, S., Nordio, G., Munz, K., Catucci, D., & Kearney, W. S. (2019). Variations in Persistence and
592 Regenerative Zones in Coastal Forests Triggered by Sea Level Rise and Storms. *Remote Sensing*, 11(17).

593 • Fernandes, A., Rollinson, C. R., Kearney, W. S., Dietze, M. C., & Fagherazzi, S. (2018). Declining radial
594 growth response of coastal forests to hurricanes and nor'easters. *Journal of Geophysical Research: Biogeosciences*, 123(3), 832-849.

595 • Fofonoff, N. P., & Millard Jr, R. C. (1983). Algorithms for the computation of fundamental properties of
596 seawater.

597 • Gardner, L. R., Michener, W. K., Williams, T. M., Blood, E. R., Kjerve, B., Smock, L. A., ... & Gresham, C.
598 (1992). Disturbance effects of Hurricane Hugo on a pristine coastal landscape: North Inlet, South Carolina,
599 USA. *Netherlands Journal of Sea Research*, 30, 249-263.

600 • Gardner, L. R., Reeves, H. W., & Thibodeau, P. M. (2002). Groundwater dynamics along forest-marsh
601 transects in a southeastern salt marsh, USA: Description, interpretation and challenges for numerical
602 modeling. *Wetlands Ecology and Management*, 10(2), 143-157.

603 • Gleeson, T., Marklund, L., Smith, L., & Manning, A. H. (2011). Classifying the water table at regional to
604 continental scales. *Geophysical Research Letters*, 38(5).

605 • Hargreaves, G. H., & Allen, R. G. (2003). History and evaluation of Hargreaves evapotranspiration
606 equation. *Journal of Irrigation and Drainage Engineering*, 129(1), 53-63.

607 • Hasegawa, P. M., Bressan, R. A., Zhu, J. K., & Bohnert, H. J. (2000). Plant cellular and molecular
608 responses to high salinity. *Annual review of plant biology*, 51(1), 463-499.

609 • Hester, M. W., Mendelsohn, I. A., & McKee, K. L. (2001). Species and population variation to salinity
610 stress in *Panicum hemitomon*, *Spartina patens*, and *Spartina alterniflora*: morphological and physiological
611 constraints. *Environmental and Experimental Botany*, 46(3), 277-297.

612 • Horton, R. E. (1933). The role of infiltration in the hydrologic cycle. *Eos, Transactions American*
613 *Geophysical Union*, 14(1), 446-460.

614 • Jarraya Horriche, F., & Benabdallah, S. (2020). Assessing aquifer water level and salinity for a managed
615 artificial recharge site using reclaimed water. *Water*, 12(2), 341.

616 • Kearney, W. S., Fernandes, A., & Fagherazzi, S. (2019). Sea-level rise and storm surges structure coastal
617 forests into persistence and regeneration niches. *PloS one*, 14(5).

618 • Kirwan, M. L., & Gedan, K. B. (2019). Sea-level driven land conversion and the formation of ghost
619 forests. *Nature Climate Change*, 9(6), 450-457.

620 • Kirwan, M. L., Temmerman, S., Skeehan, E. E., Guntenspergen, G. R., & Fagherazzi, S. (2016).
621 Overestimation of marsh vulnerability to sea level rise. *Nature Climate Change*, 6(3), 253-260.

622 • Kutílek, M., & Nielsen, D. R. (1994). Soil hydrology: textbook for students of soil science, agriculture,
623 forestry, geoecology, hydrology, geomorphology and other related disciplines. Catena Verlag.

624 • Li, L., Barry, D. A., Stagnitti, F., & Parlange, J. Y. (1999). Submarine groundwater discharge and associated
625 chemical input to a coastal sea. *Water Resources Research*, 35(11), 3253-3259.

626 • Maggard, A., Will, R., Wilson, D., & Meek, C. (2016). Response of mid-rotation loblolly pine (*Pinus taeda*
627 L.) physiology and productivity to sustained, moderate drought on the western edge of the
628 range. *Forests*, 7(9), 203.

629 • May, C. (2020). Rising groundwater and sea-level rise. *Nature Climate Change*, 10(10), 889-890.

630 • McFarland, R. E., & Scott, B. T. (2006). The Virginia coastal plain hydrogeologic framework (No. 1731).

631 • Michael, H. A., Mulligan, A. E., & Harvey, C. F. (2005). Seasonal oscillations in water exchange between
632 aquifers and the coastal ocean. *Nature*, 436(7054), 1145-1148.

633 • Michael, H. A., Russoniello, C. J., & Byron, L. A. (2013). Global assessment of vulnerability to sea-level
634 rise in topography-limited and recharge-limited coastal groundwater systems. *Water Resources*
635 *Research*, 49(4), 2228-2240.

636 • Miller, K. G., Kopp, R. E., Horton, B. P., Browning, J. V., & Kemp, A. C. (2013). A geological perspective
637 on sea-level rise and its impacts along the US mid-Atlantic coast. *Earth's Future*, 1(1), 3-18.

638 • Mohamed, A. A., Sasaki, T., & Watanabe, K. (2000). Solute transport through unsaturated soil due to
639 evaporation. *Journal of Environmental Engineering*, 126(9), 842-848.

640

- 641 • Munns, R., & Tester, M. (2008). Mechanisms of salinity tolerance. *Annu. Rev. Plant Biol.*, 59, 651-681.
- 642 • Nawaz, K., Hussain, K., Majeed, A., Khan, F., Afghan, S., & Ali, K. (2010). Fatality of salt stress to plants: 643 Morphological, physiological and biochemical aspects. *African Journal of Biotechnology*, 9(34).
- 644 • Oki, T., & Kanae, S. (2006). Global hydrological cycles and world water resources. *science*, 313(5790), 645 1068-1072.
- 646 • Or, D., & Lehmann, P. (2019). Surface evaporative capacitance: How soil type and rainfall characteristics 647 affect global-scale surface evaporation. *Water Resources Research*, 55(1), 519-539.
- 648 • Pezeshki, S. R., DeLaune, R. D., & Patrick Jr, W. H. (1990). Flooding and saltwater intrusion: potential 649 effects on survival and productivity of wetland forests along the US Gulf Coast. *Forest Ecology and 650 Management*, 33, 287-301.
- 651 • Poljakoff-Mayber, A., & Gale, J. (Eds.). (1975). *Plants in saline environments* (p. 213). New York: 652 Springer-verlag.
- 653 • Rice, D., & Rooth, J. (2000). Colonization and expansion of *Phragmites australis* in upper Chesapeake Bay 654 tidal marshes. *Wetlands*, 20(2), 280-299.
- 655 • Richter, B. C., & Kreitler, C. W. (1993). Geochemical techniques for indentifying sources of groundwater 656 salinization: Boca Raton. FL, CK Smoley, 258.
- 657 • Robinson, C., Li, L., & Barry, D. A. (2007). Effect of tidal forcing on a subterranean estuary. *Advances in 658 Water Resources*, 30(4), 851-865.
- 659 • Rotzoll, K., & Fletcher, C. H. (2013). Assessment of groundwater inundation as a consequence of sea-level 660 rise. *Nature Climate Change*, 3(5), 477-481.
- 661 • Sallenger, A. H., Doran, K. S., & Howd, P. A. (2012). Hotspot of accelerated sea-level rise on the Atlantic 662 coast of North America. *Nature Climate Change*, 2(12), 884-888.
- 663 • Schuerch, M., Spencer, T., Temmerman, S., Kirwan, M. L., Wolff, C., Lincke, D., ... & Brown, S. (2018). 664 Future response of global coastal wetlands to sea-level rise. *Nature*, 561(7722), 231-234.
- 665 • Stanturf, J. A., Goodrick, S. L., & Outcalt, K. W. (2007). Disturbance and coastal forests: a strategic approach 666 to forest management in hurricane impact zones. *Forest Ecology and Management*, 250(1-2), 119-135.
- 667 • Sumner, D. M., & Belaineh, G. (2005). Evaporation, precipitation, and associated salinity changes at a humid, 668 subtropical estuary. *Estuaries*, 28(6), 844-855.
- 669 • Taniguchi, M., Burnett, W. C., Cable, J. E., & Turner, J. V. (2002). Investigation of submarine groundwater 670 discharge. *Hydrological Processes*, 16(11), 2115-2129.
- 671 • Thibodeau, P. M., Gardner, L. R., & Reeves, H. W. (1998). The role of groundwater flow in controlling the 672 spatial distribution of soil salinity and rooted macrophytes in a southeastern salt marsh, USA. *Mangroves and Salt Marshes*, 2(1), 1-13.
- 673 • Thornthwaite, C. W. (1948). An approach toward a rational classification of climate. *Geographical 674 review*, 38(1), 55-94.
- 675 • Trajkovic, S. (2005). Temperature-based approaches for estimating reference evapotranspiration. *Journal of 676 irrigation and drainage engineering*, 131(4), 316-323.
- 677 • Trajkovic, S. (2007). Hargreaves versus Penman-Monteith under humid conditions. *Journal of Irrigation 678 and Drainage Engineering*, 133(1), 38-42.
- 679 • Tully, K., Gedan, K., Epanchin-Niell, R., Strong, A., Bernhardt, E. S., BenDor, T., ... & Weston, N. B. 680 (2019). The invisible flood: The chemistry, ecology, and social implications of coastal saltwater 681 intrusion. *BioScience*, 69(5), 368-378.
- 682 • Werner, A. D., Bakker, M., Post, V. E., Vandenbohede, A., Lu, C., Ataie-Ashtiani, B., ... & Barry, D. A. 683 (2013). Seawater intrusion processes, investigation and management: recent advances and future 684 challenges. *Advances in water resources*, 51, 3-26.
- 685 • Williams, K., Ewel, K. C., Stumpf, R. P., Putz, F. E., & Workman, T. W. (1999). SEA-LEVEL RISE AND 686 COASTAL FOREST RETREAT ON THE WEST COAST OF FLORIDA, USA. *Ecology*, 80(6), 2045-687 2063.
- 688 • Wilson, A. M., Evans, T., Moore, W., Schutte, C. A., Joye, S. B., Hughes, A. H., & Anderson, J. L. (2015). 689 Groundwater controls ecological zonation of salt marsh macrophytes. *Ecology*, 96(3), 840-849.
- 690 • Xie, H., Yi, Y., Hou, C., & Yang, Z. (2020). In situ experiment on groundwater control of the ecological 691 zonation of salt marsh macrophytes in an estuarine area. *Journal of Hydrology*, 585, 124844.

693 • Yan, S. F., Yu, S. E., Wu, Y. B., Pan, D. F., & Dong, J. G. (2018). Understanding groundwater table using
694 a statistical model. *Water Science and Engineering*, 11(1), 1-7.
695 • Yan, S. F., Yu, S. E., Wu, Y. B., Pan, D. F., She, D. L., & Ji, J. (2015). Seasonal variations in groundwater
696 level and salinity in coastal plain of eastern China influenced by climate. *Journal of Chemistry*, 2015.
697 • Yates, D., & Strzepek, K. M. (1994). Potential evapotranspiration methods and their impact on the
698 assessment of river basin runoff under climate
699 •

700